Published by IOP Publishing for Sissa Medialab

Received: *October 19, 2023*
Accepted: *December 29, 2023*
Published: *March 12, 2024*

24th International Workshop on Radiation Imaging Detectors
Oslo, Norway
25–29 June 2023

A simulator for Timepix-like pixel front-ends

R. Ballabriga Sune,[a] **H. Bromberger,**[b] **M. Campbell,**[a] **X. Llopart Cudie,**[a] **P. Christodoulou,**[a,c] **V. Sriskaran**[a] **and L. Tlustos**[a,c,*]

[a] *EP, CERN,*
1211 Geneva 23, Switzerland
[b] *CFEL, DESY,*
Notkestr. 85, 22607 Hamburg, Germany
[c] *IEAP, CTU,*
Husova 240/5, 110 00 Prague 1, Czech Republic

E-mail: lukas.tlustos@cern.ch

Abstract: This work presents the development of a front-end simulation code for the Timepix3 readout chip [1], intended as digitizer stage in full detector simulation. The front-end electronics is modelled using an integrator stage and 3 parallel feedback loops with individually configurable time constants. The main feedback discharging the integrator consists of 3 low-pass filtered feedback loops. The leakage current compensation is approximated by an additional independent low-pass filtered feed-back loop. The system noise is modelled using independent bandwidth limited noise channels for pre-amplifier, feedback and threshold noise. The Timepix3 time of arrival (ToA) and time over threshold (ToT) measurement is implemented by a discriminator model with independent rise and fall times and 2 independent clock frequencies for ToA and ToT. The measured dependence of the ToT on the pre-amplifier input charge using test-pulses of a Timepix3 assembly is correctly reproduced for a wide range of discriminator settings.

Keywords: Detector modelling and simulations I (interaction of radiation with matter, interaction of photons with matter, interaction of hadrons with matter, etc); Simulation methods and programs; Solid state detectors; Hybrid detectors

*Corresponding author.

https://doi.org/10.1088/1748-0221/19/03/C03022

2024 JINST 19 C03022

Contents

1 Introduction

Detector simulation is an important tool to understand and validate experimental results. With the ground truth data included in the data set, a sufficiently realistic detector model is very valuable in the development and validation of track and particle reconstruction algorithms. In order to correctly describe the behaviour of the full detector system, charge deposition, charge transport and the pixel front-end electronics need to be accurately modelled. In this work, a simulation code for pixel front-end electronics employing the Krummenacher feedback loop system has been developed and tuned to the characteristics of the Timepix3 [1] ASIC (Application Specific Integrated Circuit).

2 Implementation

The Timepix3 pixel CSA (Charge Sensitive Amplifier) is implemented using the Krummenacher feedback architecture [2, 3], a simplified schematics is given in figure 1(a). The incoming current pulse is converted into a triangular voltage pulse at the output of the preamplifier which is then compared against a threshold voltage. In the Timepix3 chip, this reference level is globally set for the pixel matrix using a tunable DAC (Digital-to-Analog Converter) located in the chip periphery [1]. The DAC response has to be calibrated in order to be correctly set to a given charge threshold. In the same way also the discharge time which is controlled by the magnitude of the preamplifier discharge current is regulated via a dedicated 8-bit DAC.

The presented model aims to phenomenologically reproduce the behaviour of the pixel front-end and the computation entirely stays in the charge domain. In this way the model parameters such as discriminator threshold and discharge current are also kept in physical units of charge and time. The schema of the computational model is shown in figure 1(b). The pixel front-end is composed of an integrator stage and parallel feedback loops with individually configurable time constants. The main feedback discharging the integrator consists of 3 parallel weighted loops, each implemented as a first order Butterworth filter. The time constant of the first feedback branch is in the order of 50 ns, representing the main discharge pole in the feedback loop [3]. In order to reproduce the measured

behaviour of the Timepix3, two additional poles had to be added: a complex conjugate pole with a time constant of ~350 ns, resulting in a small oscillation in the undershoot of the output signal. And a second simple pole with a longer time constant of ~2.5 µs, providing a better approximation of the amplitude of the undershoot, see figure 2. The leakage current compensation (LCC) is approximated by an additional independent low-pass filtered feed-back loop with a much longer time constant of 10 µs. The sum of the discharge loop and the leakage current compensation loop cannot exceed the maximum discharge current, which corresponds to half the reset Krummenacher current in the actual pixel circuit [3, 4]. The system noise is implemented using independent bandwidth limited noise channels for pre-amplifier and feedback loops with configurable values for bandwith and equivalent noise charge (ENC) r.m.s.

The ToA (Time of Arrival) and ToT (Time over Threshold) simulation is performed by a discriminator model with independent rise and fall times, comparing Q_{out} in figure 1(b) against the discriminator threshold. Since the effective threshold in the Timepix3 is set via the difference between two voltage DACs, a bandwidth limited noise of 7 e- is added to the discriminator threshold level. The discriminator uses two independent clocks of 25 ns and 1.56 ns, corresponding to 40 and 640 MHz respectively, to determine the ToT and ToA values accordingly.

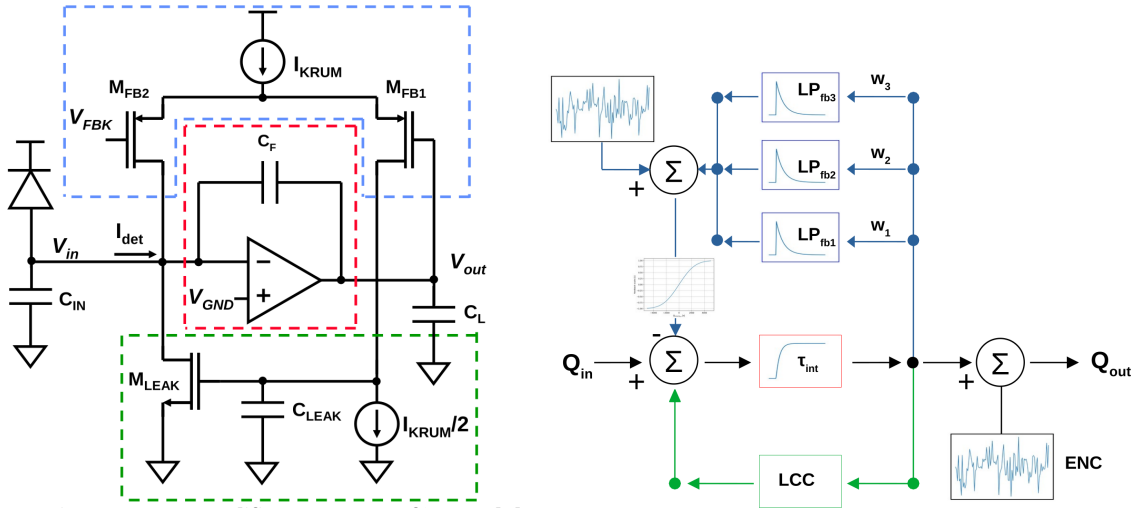

(a) Simplified schematic of the Timepix3 preamplifier [3].

(b) Schematic of the preamplifier model

Figure 1. The schematic of the circuit (a) and the model (b): the CSA in red is modelled as a integrator stage. The discharge of the integrator stage takes place via 3 independent low-pass filtered feedback loops in blue. In addition the leakage current compensation is implemented as low-pass filter with a cut-off frequency of ~10 kHz, in green. As opposed to the signals in the real circuit, the whole simulation is performed in charge domain. Two configurable band-width limited noise sources are added, a feedback current noise and preamplifier output noise ENC.

In order to obtain this behaviour with a simple computational model, the integrator and low- and band-pass pass filters are implemented as discrete transfer functions [5]

$$h(z) = A\frac{\prod_i^M (z - q_i)}{\prod_j^N (y_j - p_j)} \tag{2.1}$$

$$y_n = \frac{1}{a_0} \cdot \left[\sum_{i=0}^{M} b_i \cdot x_{n-i} - \sum_{j=1}^{N} a_j \cdot y_{n-j} \right] \tag{2.2}$$

2024 JINST 19 C03022

with b_i the feed-forward scaling and with a_j the feed-backward scaling parameters, respectively the zeros q_i and poles p_j of the filters in the z-domain. In order to reduce computational load the transfer function is set to idle and returns zero without further calculations when all x_{n-i} and y_{n-j} are below a cut-off threshold.

For small input signals, here in the order of below ~1 ke-, the front-end electronics channel can approximately be modelled by convoluting the input current with the small signal impulse response [3]

$$Q_{\text{out}}(t) = Q_{\text{in}}(t) \otimes \frac{\exp(-t/\tau_{\text{rise}}) - \exp(-t/\tau_{\text{fall}})}{\tau_{\text{rise}} - \tau_{\text{fall}}},$$

with τ_{rise} and τ_{fall} the rise time and fall time constants. In this small signal representation the RT0 time (Return to Zero) of the front-end output time is constant, independent of the magnitude of the input charge. However, in a Krummenacher circuit the feedback current saturates for larger input charges and the RT0 increases linearly with the total input charge. Of particular impact for the dependence of the ToT on the total input charge is the transition between small signal regime (where the RT0 is constant) and the feedback saturation regime (where the discharge current is constant). This is achieved by tapering the nominal feedback current I_{max} [6], approximating a constant fraction discharge below a configurable small signal limit a as

$$I_{\text{feedback}} = I_{\text{max}} \cdot \tanh\left(\frac{Q_{\text{out}}}{a}\right) \tag{2.3}$$

The effect of this feedback tapering can be seen in figure 2, both in the signal shape and in the dependence of the ToT on the input charge. The charge vs ToT simulation on the right hand side of figure 2 shows a characteristic knee at input charges around 1 ke-, below which the ToT stays approximately constant for discriminator thresholds lower than the small signal limit, whereas the ToT increase becomes linear at higher input charges.

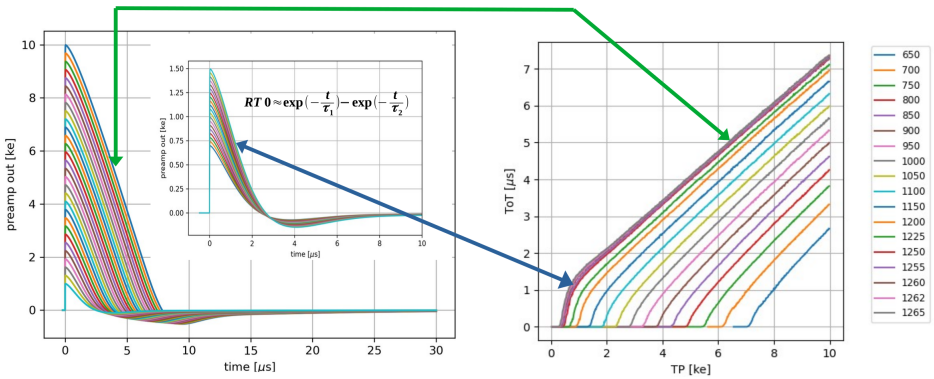

Figure 2. Left: preamplifier output current for input charges from 700 e- to 10 ke-. Right: the dependence of the ToT on the input charge for discriminator thresholds from ~400 e- to ~700 ke-. Please note that this simulation does not include any noise contributions.

Figure 3 shows the time series of the preamplifier output, threshold, discriminator and the feedback currents for a 10 ke- input pulse and 10 e-/ns discharge current. The preamplifier noise ENC was set to 60 e- r.m.s and the feedback current noise ENC to 0.01 e-/ns r.m.s. The undershoot caused by the complex conjugate pole is clearly visible as well as the small offset with slow recovery due to the leakage current compensation.

2024 JINST 19 C03022

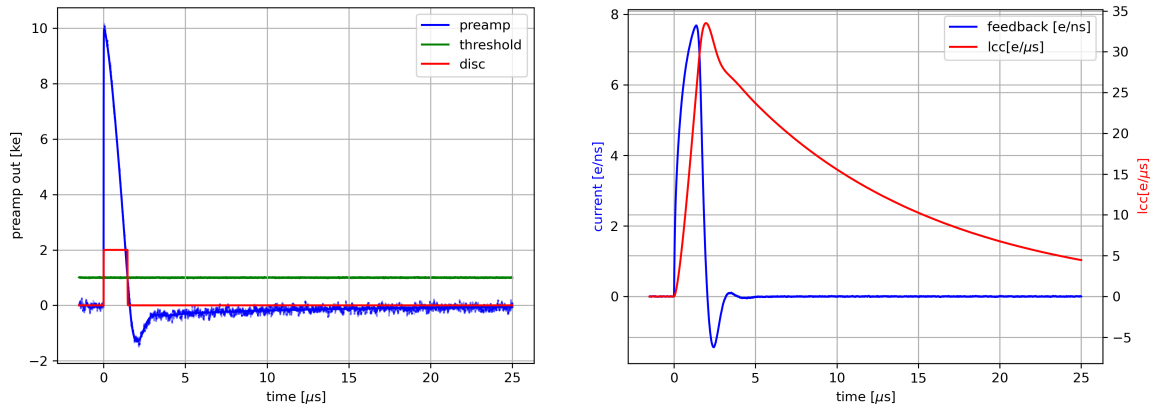

(a) (b)

Figure 3. a) The simulated preamplifier output for a 10 ke- input charge, together with the discriminator threshold and the discriminator output. b) The feedback current and the contribution from the LCC with a time constant of ~10 µs. The bandwidth filtered noise on the feedback current has 0.01 e-/ns r.m.s. Please note the different scales for feedback current and leakage current compensation.

3 Parameter tuning

3.1 ToT calibration

The model parameter were tuned to reproduce the ToT calibration curve, given by the dependence of the ToT on input charge. ToT calibration curve was measured using test-pulses in a single pixel of a Timepix3 assembly for discriminator thresholds from ~500 e- to ~7 ke-. The input charge range was scanned in steps of 18.8 e- in the range of 500 e- to 10 ke-. The model parameters were selected such that a peaking time of the preamplifier output of 35 ns was obtained. The relative weights of the feedback branches were found using a least square fit to the measured ToT calibration curves. The resulting simulated ToT calibration curves are in very good agreement with test pulse measurements, lying within the 1 σ margin of the measurement, see figure 4.

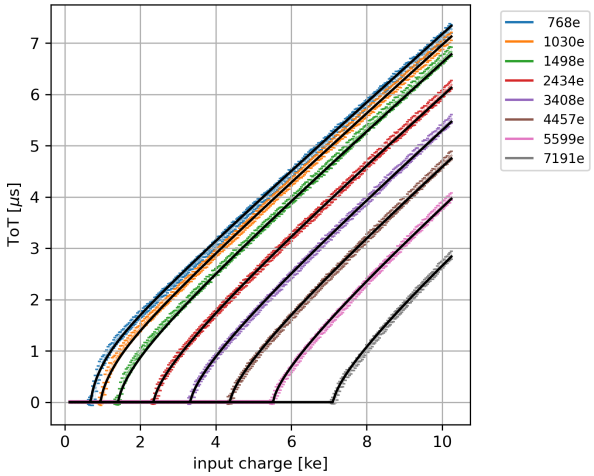

Figure 4. The ToT calibration of a single Timepix3 pixel measured using test pulse overlaid with corresponding simulated ToT values (black lines) for discriminator thresholds from 768 e- to 7.2 ke-. The measured ToT calibration is plotted with 1 σ error margins.

2024 JINST 19 C03022

4 Results

4.1 ToA and timewalk

While three configurable clock periods can be simulated, in this example only two are used, namely 25 ns and 1.56 ns like in the Timepix3. Figure 5 shows the simulated ToA for input charge values ranging from the used threshold level of 2.9 ke- to 10 ke-. The result is consistent with published results [7, 8]. Also visible is the effect of the system noise of 80 e- ENC r.m.s, 7 e- r.m.s threshold noise and the long peaking time of the Timepix3 of ~35 ns for low charge inputs. The strong impact of the noise on the precision of the ToA measurement for lower input charges is clearly visible. While for e.g. 9 ke- input pulse only two ToA values are measured, at 3 ke- the measured ToA spreads over 5 values, figure 5(b).

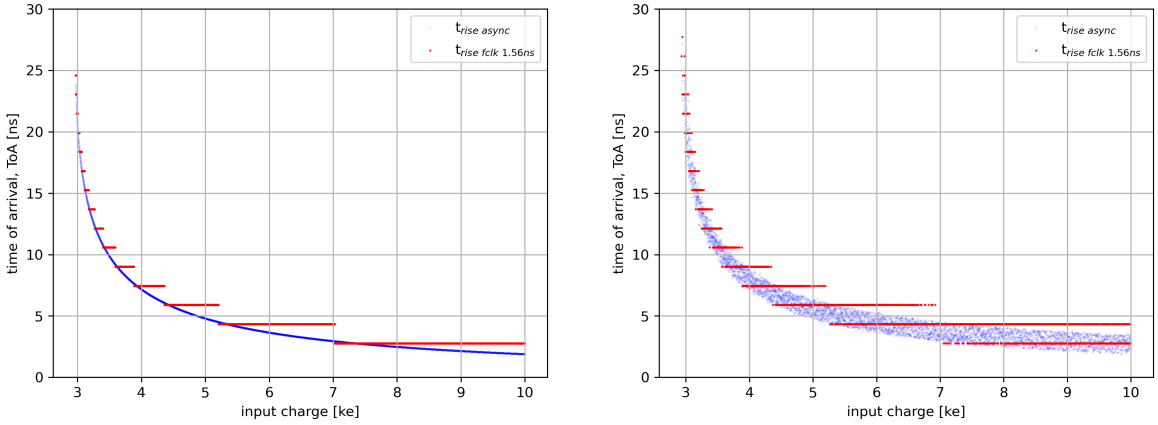

Figure 5. a) The simulated timewalk without noise. The simulated ToA values are well separated within the bins of 1.56 ns. b) The simulated timewalk with 60 e- ENC preamplifier noise. The significant overlap of measured ToA especially for low input charges is clearly visible.

4.2 Pulse pileup

Double LED pulse measurements performed at DESY showed a reduction of measured ToT for the second LED pulse with decreasing interval between the pulses [9], indicating an effect of pulse pileup. This reduction could be reproduced very well by the simulation and is shown to be a consequence of the signal undershoot following a big input charge. Figure 6(a) shows a trail of 2 pulses of 5 ke- input charge spaced in time by 2 µs. Since the second pulse is injected while the preamplifier output is still in the undershoot stemming from the first pulse, the second output pulse starts from a negative offset and the integral feedback also includes contributions from the feedback branches with longer time constant originating in the first pulse. Consequently both the amplitude and the RT0 time of the second pulse are reduced.

Figure 6(b) plots the measured ToT of the second pulse in dependence of the delay between the LED pulses, together with the results of the corresponding simulation. The model reproduces the experimental results for delays longer than ~2.5 µs, however for shorter delays experiment and simulation start to deviate significantly. The model can be tuned such that the experimental results are reproduced over the whole range, but this comes at the cost of increased deviations from the measured ToT calibration in figure 4. The reason for this lies in the fact that the model uses fixed time constants

2024 JINST 19 C03022

and fixed relative weights for the feedback branches, which is not the case for the real pixel front-end where both dynamically change with the front-end charge load. The correct modelling of the drift of time constants and weights is beyond the scope of this work and will be addressed in future.

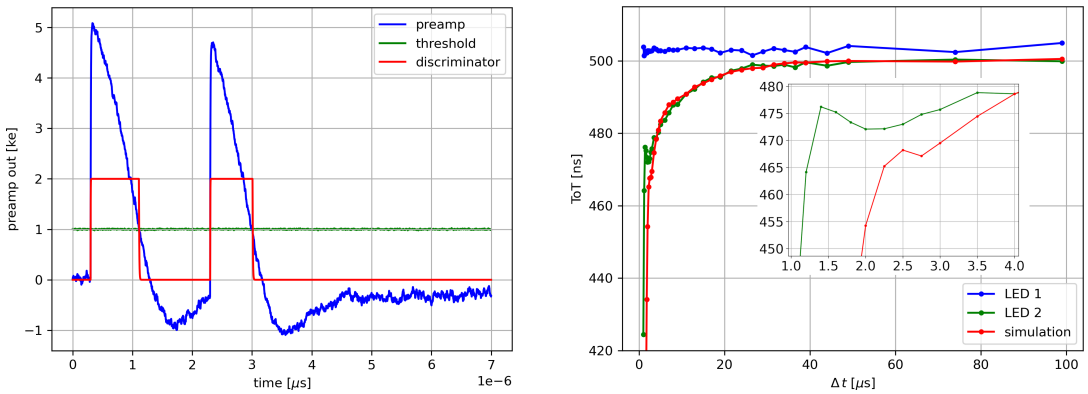

(a) (b)

Figure 6. a) The simulation of two 5 ke- input pulses with a delay of 2 µs. b) The measured and simulated reduction of the ToT in dependence on the delay of the second pulse with respect to first pulse. Below ~2.5 µs the simulation deviate from the experimental results.

4.3 X-ray fluorescence

In figure 7 the simulated ToT spectrum for an irradiation with a 241Am γ source is plotted. For this simulations the model has been ported to the Allpix2 framework [10]. The actual detector geometry of the experimental Timepix3 device, with the Si sensor thickness of 500 µm and 200 V sensor bias, has been replicated in the simulation. Since for the per-pixel ToT calibration using monochromatic X-rays only single pixel events are used, also in this case only single pixel events are taken into account. The value for the feedback current used in the simulation was chosen such that the mean ToT value is equal in measurements and simulations. The width of the simulated spectrum is in good agreement with the experimental values for a feedback current values generally used for γ measurements, see figure 7(b).

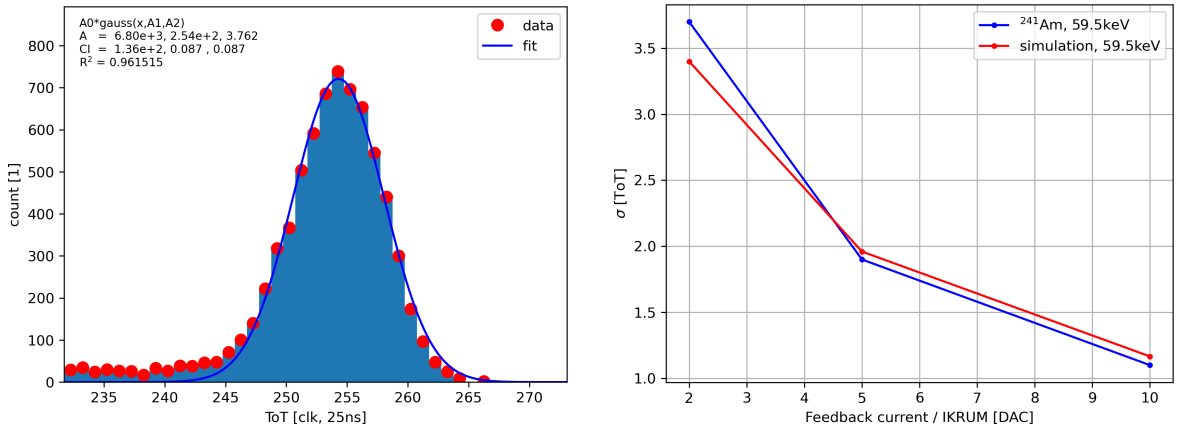

(a) (b)

Figure 7. a) Measured 59.5 keV fluorescence line with low feedback current (I_{Krum} = 2). b) Measured and simulated spectral resolution dependence on the feedback current.

2024 JINST 19 C03022

5 Summary

A numerical model for Timepix-like pixel front-ends has been developed. For the sake of simplicity and computational performance the time constants and relative weights in the model are fixed and do not depend on the charge load of the front-end. The model is also available as plug-in [11] for the Allpix2 framework. It reproduces very well the experimental results of ToT calibration, ToA dependency and spectral response to monochromatic X-rays over a wide range of discriminator threshold and feedback current values. The pileup simulation shows deviations for high input charges and high feedback currents for pulse intervals below 2.5 µs. This deviation is due to the fixed values for the time constants and relative weights, and in particular of the complex conjugate pole present in the Timepix3. Since the model is highly configurable it can and will be adapted to other pixel front-end such as the Timepix2 [12] and Timepix4 [13].

Acknowledgments

The authors acknowledge funding from CERN Medical Applications and the Medipix3 collaboration.

References

[1] A. Kruth et al., *Timepix3: a 65K channel hybrid pixel readout chip with simultaneous ToA/ToT and sparse readout*, 2014 *JINST* **9** C05013.

[2] F. Krummenacher, *Pixel detectors with local intelligence: an IC designer point of view*, *Nucl. Instrum. Meth. A* **305** (1991) 527.

[3] R. Ballabriga, *The Design and Implementation in 0.13um CMOS of an Algorithm Permitting Spectroscopic Imaging with High Spatial Resolution for Hybrid Pixel Detectors*, Ph.D. Thesis, CERN (2009).

[4] M. De Gaspari et al., *Design of the analog front-end for the Timepix3 and Smallpix hybrid pixel detectors in 130 nm CMOS technology*, 2014 *JINST* **9** C01037.

[5] S. Hollos and J.R. Hollos, *Recursive Digital Filters: A Concise Guide*, Abrazol Publishing (2014).

[6] J. Kaplon, *Krummenacher loop for large signal*, https://jkaplon.web.cern.ch/Krumenacher/Krumenacher_closeloopLargeSignal.pdf.

[7] S. Tsigaridas et al., *Timewalk correction for the Timepix3 chip obtained with real particle data*, *Nucl. Instrum. Meth. A* **930** (2019) 185 [arXiv:1902.00480].

[8] D. Turecek, J. Jakubek and P. Soukup, *USB 3.0 readout and time-walk correction method for Timepix3 detector*, 2016 *JINST* **11** C12065.

[9] H. Bromberger, D. Pennicard, R. Ballabriga, J. Küpper and S. Trippel, *Timepix3: single pixel, multi hit intensity behaviour*, in preparation (2023).

[10] S. Spannagel et al., *Allpix^2: A Modular Simulation Framework for Silicon Detectors*, *Nucl. Instrum. Meth. A* **901** (2018) 164 [arXiv:1806.05813].

[11] L. Tlustos, *TpxDigitizer*, https://gitlab.cern.ch/ltlustos/TpxDigitizer_AP2 (2023).

[12] W.S. Wong et al., *Introducing Timepix2, a frame-based pixel detector readout ASIC measuring energy deposition and arrival time*, *Radiat. Meas.* **131** (2020) 106230.

[13] R. Ballabriga et al., *The Timepix4 analog front-end design: Lessons learnt on fundamental limits to noise and time resolution in highly segmented hybrid pixel detectors*, *Nucl. Instrum. Meth. A* **1045** (2023) 167489.

2024 JINST 19 C03022